This paper is available on line at http://www.mcponline.org

Proteomic Analysis of Temporally Stimulated Ovarian Cancer Cells for Biomarker Discovery*[S]

Mark A. Marzinke‡, Caitlin H. Choi‡, Li Chen‡, Ie-Ming Shih‡, Daniel W. Chan‡, and Hui Zhang‡§

While ovarian cancer remains the most lethal gynecological malignancy in the United States, there are no biomarkers available that are able to predict therapeutic responses to ovarian malignancies. One major hurdle in the identification of useful biomarkers has been the ability to obtain enough ovarian cancer cells from primary tissues diagnosed in the early stages of serous carcinomas, the most deadly subtype of ovarian tumor. In order to detect ovarian cancer in a state of hyperproliferation, we analyzed the implications of molecular signaling cascades in the ovarian cancer cell line OVCAR3 in a temporal manner, using a mass-spectrometry-based proteomics approach. OVCAR3 cells were treated with EGF[1], and the time course of cell progression was monitored based on Akt phosphorylation and growth dynamics. EGF-stimulated Akt phosphorylation was detected at 12 h post-treatment, but an effect on proliferation was not observed until 48 h post-exposure. Growth-stimulated cellular lysates were analyzed for protein profiles between treatment groups and across time points using iTRAQ labeling and mass spectrometry. The protein response to EGF treatment was identified via iTRAQ analysis in EGF-stimulated lysates relative to vehicle-treated specimens across the treatment time course. Validation studies were performed on one of the differentially regulated proteins, lysosomal-associated membrane protein 1 (LAMP-1), in human tissue lysates and ovarian tumor tissue sections. Further, tissue microarray analysis was performed to demarcate LAMP-1 expression across different stages of epithelial ovarian cancers. These data support the use of this approach for the efficient identification of tissue-based markers in tumor development related to specific signaling pathways. LAMP-1 is a promising biomarker for studies of the progression of EGF-stimulated ovarian cancers and might be useful in predicting treatment responses involving tyrosine kinase inhibitors or EGF receptor monoclonal antibodies. ***Molecular & Cellular Proteomics 12: 10.1074/mcp.M112.019521, 356–368, 2013.***

Ovarian cancer is the leading cause of death from gynecologic malignancy in the United States, and the fifth leading cause of cancer-related deaths in women (1). Epithelial ovarian cancers are extensively heterogeneous; histological subclassification by cell type includes serous, endometrioid, clear-cell, mucinous, transitional, squamous, and undifferentiated (2). Serous epithelial cancers are the most commonly diagnosed epithelial ovarian cancer subtype and are associated with the majority of ovarian-cancer-related deaths (1).

From a molecular perspective, the basic characteristic of any cancerous cell is its ability to grow uncontrollably. As a cell proliferates, a cascade of molecular and morphological changes occurs, including the activation of signaling cascades that modulate cytoskeletal dynamics, cell cycle progression, and angiogenesis (3–5). In addition to the unrestrained aberrant proliferation of cancer cells, other processes are required for disease progression, including changes in cellular adhesion to endothelial cells and in the extracellular microenvironment (6). It is important to note, however, that cancer cell progression is not an instantaneous event, and the demarcation between non-cancer and cancer is not static. It is postulated that epithelial cancer cells transition to a highly motile and invasive mesenchymal cell type, and this epithelial-to-mesenchymal transition is a critical molecular mechanism in tumor progression and metastasis (6). Several important signaling cascades have been implicated in this transition, including those mediated by EGF, PDGF, and TGFβ and those involving PI3K/Akt activation (7, 8). Thus, biomarkers of cancer progression can serve as indicators of disease etiology and potential staging, as well as predictive markers of therapeutic regimen responses. The identification of differentially expressed proteins during cancer metastasis has the potential to be utilized both prognostically with regard to metastatic development and predictively, through the implementation of pathway-specific therapies.

From the ‡Department of Pathology, Johns Hopkins University, Baltimore, MD 21231

Received April 23, 2012, and in revised form, November 3, 2012
Published, MCP Papers in Press, DOI 10.1074/mcp.M112.019521

[1] The abbreviations used are: EGF, epidermal growth factor; EGFR, epidermal growth factor receptor; FIGO, International Federation of Gynecology and Obstetrics; iTRAQ, isobaric tags for relative and absolute quantitation; LAMP-1, lysosomal-associated membrane protein 1; pAkt, phospho-Akt; PI3K, phosphatidylinositol 3-kinase; LTQ, linear trap quadrupole; MS, mass spectrometry; MTT, 3-(4,5-dimethylthiazol-2-yl)-2,5-diphenyltetrazolium bromide; TMA, tissue microarray; TKI, tyrosine kinase inhibitor.

Molecular analyses indicate the oncogenic role of the epidermal growth factor receptor (EGFR) in several human cancers, including lung cancers and *Her2*-amplified breast cancers (9). However, less is known regarding the implications of aberrant EGFR expression in ovarian cancer progression, particularly in terms of increased activation of downstream signaling cascades and efficacious therapeutic regimens. Studies illustrate overamplification of the *EGFR* gene in between 4% and 22% of ovarian cancers, with aberrant protein expression in up to 60% of ovarian malignancies (10–12). Aberrant EGFR expression has been associated with high tumor grade, increased cancerous cell proliferation, and poorer patient outcomes (12–15). Gene amplification and the overexpression of other EGFR family members such as *Her2* and *ErbB3* have also been reported in epithelial ovarian cancers (15). Further, studies performed *in vitro* illustrate the ability of EGF to induce DNA synthesis and stimulate cell growth in OVCAR3 cells (16).

Although EGFR and downstream EGF-regulated signaling cascades have been implicated in ovarian malignancies, the treatment of ovarian tumors with anti-EGFR agents has induced minimal response. Targeted EGFR therapies fall into two categories: monoclonal antibodies that target the receptor extracellular domain to prevent ligand binding, and tyrosine kinase inhibitors (TKIs), which aim to prevent the activation of downstream signaling cascades. Although EGFR inhibitors exhibit modest success *in vitro*, no agents have been approved by the U.S. Food and Drug Administration for the treatment of malignant ovarian tumors (17). Among other therapeutic approaches, studies have looked at the potential efficacy of the TKIs erlotinib and gefitinib in the treatment of ovarian cancers; unfortunately, neither drug was effective in eliciting a significant response in ovarian tumor treatment (12, 15, 18, 19). However, the identification of markers of pathway-stimulated processes might help to stratify disease and select patients with EGF signaling activation. The identified markers might facilitate the prediction of treatment responses.

MS-based proteomic studies have been heavily implemented in the identification of candidate biomarkers in a variety of specimen sources ranging from epithelial ovarian cancer tissue to immortalized cell lines and cultured media (20–22). The human adenocarcinoma OVCAR3 cell line is derived from an epithelial ovarian cancer with a high grade serous cell type and exhibits many of the molecular and morphological aspects of serous epithelial cancers (23, 24). This cell line can be stimulated to promote or inhibit cellular proliferation using various molecular agonists and antagonists (23–25). Because of the molecular and morphological similarities between the OVCAR3 cell line and ovarian adenocarcinoma cells, it serves as an appropriate high-throughput surrogate for candidate biomarker identification. Further, the analysis of a single cell line allows for the identification of temporal protein regulation within a single homogeneous cell population using an orthogonal approach.

In the present study, the OVCAR3 cell line was treated with the hyperproliferative molecule EGF or the PI3K/Akt inhibitor LY294002 over a 48-h time course. Three time points were analyzed for biochemical and molecular changes, including Akt phosphorylation status and increased proliferation. Additionally, growth-stimulated and growth-inhibited cellular lysates were analyzed using quantitative proteomics with iTRAQ and MS/MS, and these analyses illustrated comparable global protein profiles between treatment groups and across time points. Differentially expressed proteins were identified in growth-stimulated cells as opposed to control (vehicle-treated) cells. One of the differentially regulated proteins, lysosomal-associated membrane protein 1 (LAMP-1, also known as CD107a), was further verified via immunoblotting and immunohistochemical analyses in normal and ovarian cancer tissues, in addition to tissue microarray analysis. This study demonstrates that through the use of a growth-stimulated cell culture model using EGF, the rapid identification of differentially regulated proteins as proliferation progresses may be achieved via large-scale proteomic analyses. The identification of regulated proteins along the pathway of increased cellular growth and proliferation might serve a predictive role in treatment outcomes.

MATERIALS AND METHODS

Cell Culture—The human serous epithelial ovarian cancer cell line OVCAR3 (ATCC, Manassas, VA) was cultured at 37 °C with 5% CO_2 in RPMI 1640 media with 2 mM L-glutamine, 1.5 g/l sodium bicarbonate, 10% FBS, and 1% penicillin-streptomycin. FBS and penicillin-streptomycin were obtained from Invitrogen-Invitrogen (Grand Island, NY). All other reagents were obtained from Sigma-Aldrich (St. Louis, MO).

All compounds for cell treatments were obtained from Sigma-Aldrich. EGF was prepared as a stock solution at a concentration of 1 mg/ml in 10 mM acetic acid. The PI3K/Akt inhibitor LY294002 was prepared as a stock solution at a concentration of 25 mM in dimethyl sulfoxide (DMSO). EGF and LY294002 were used at final concentrations of 50 ng/ml and 25 μM, respectively.

For cell culture assays, OVCAR3 cells were plated in six-well plates and grown in full media containing 10% FBS. Once cells reached 70% confluency, the media was replaced with serum-free media, and cells were serum-starved for 24 h. OVCAR3 cells were then treated with EGF at a final concentration of 50 ng/ml or LY294002 at a final concentration of 25 μM. Vehicle (control)-treated cells were treated with 25 μM DMSO and 0.1 μM acetic acid. Cells were incubated for 12 to 48 h prior to collection.

Western Blot Analysis—Following incubation, media was removed and cells were rinsed twice in cold PBS. Cells were lysed on ice for 15 min in 1X radioimmunoprecipitation assay buffer (Sigma-Aldrich) containing a protease inhibitor mixture (SigmaFAST tablets, Sigma-Aldrich) with final concentrations of 2 mM 4-(2-aminoethyl) benzenesulfonyl fluoride hydrochloride, 1 mM EDTA, 130 μM bestatin, 14 μM E64, 1 μM leupeptin, and 0.3 μM aprotonin. Total protein concentrations were determined using the Pierce BCA Assay (Thermo Scientific, Rockford, IL) following the manufacturer's guidelines. Lysates were diluted 1:1 with 2X Laemmli's SDS sample buffer containing 10% β-mercaptoethanol. For immunoblotting analysis, 15 μg of total protein lysate was used for Akt, or 20 μg of total proteins was used for pAkt.

For tissue analysis using Western blot, normal and stage-specific tissue lysates were acquired from Origene Technologies (Rockville, MD). Tissue lysates analyzed included human ovary tissue protein lysate, within normal region; human ovary tissue protein lysate, adenocarcinoma of ovary, serous, International Federation of Gynecology and Obstetrics (FIGO) staging IIB, tumor-node-metastasis (TNM) staging T2b, N0, MX; human ovary tissue protein lysate, adenocarcinoma of ovary, serous, FIGO staging III, TNM staging T3, NX, MX; and human ovary tissue protein lysate, adenocarcinoma of ovary, metastatic liver, FIGO stage III, T3, NX, MX. Tissue lysates were diluted 1:1 with 2X Laemmli's buffer as previously described. For immunoblotting analysis, 10 μg of total protein lysates was used.

Cell culture and tissue lysates were resolved on 4%–12% Bis-Tris denaturing gels (Invitrogen, Carlsbad, CA) using the manufacturer's settings, and proteins were transferred to nitrocellulose. Membranes were blocked with 5% nonfat dry milk powder in PBS with 0.1% Tween-20 followed by overnight primary antibody incubation at 4 °C. Primary antibodies included affinity purified mouse monoclonal anti-LAMP-1, clone E-5 (0.5 μg/ml, Santa Cruz Biotechnologies, Santa Cruz, CA), affinity purified rabbit polyclonal anti-Akt (1:1000, Cell Signaling, Boston, MA), affinity purified rabbit polyclonal anti-pAkt (Ser473) (1:1000, Cell Signaling), and affinity purified rabbit polyclonal anti-actin (0.5 μg/ml, Sigma-Aldrich). Membranes were washed three times in PBS before being incubated with secondary antibodies conjugated to HRP (0.01 μg/ml, Thermo Scientific, Rockville, IL) in blocking buffer for 1 h. Antigen–antibody conjugates were visualized using reagents supplied in the SuperSignal West Pico or Femto Chemiluminescent kit (Thermo Scientific).

3-(4,5-dimethylthiazol-2-yl)-2,5-diphenyltetrazolium Bromide Assays—OVCAR3 cells were plated at a density of 5 to 15 $\times$ 10^3 cells/well of a 96-well plate. Forty-eight hours post-plating, media was removed and replaced with serum-free media, and 24 h later, cells were treated with vehicle, EGF, LY294002, or a combination of EGF and LY294002 for 12 h to 48 h as previously described. Cellular proliferation was determined with the use of a 3-(4,5-dimethylthiazol-2-yl)-2,5-diphenyltetrazolium bromide (MTT)-based cell growth determination kit (Sigma-Aldrich) as per the manufacturer's instructions. Briefly, 10% (v/v) of MTT solution was added per well and incubated at 37 °C and 5% CO_2 for 4 h. Cell supernatants were aspirated, and MTT precipitates were resuspended in MTT solvent for 30 min. The reconstituted precipitate was spectrophotometrically measured using a BioTek μQuant (Winooski, VT) microtiter plate reader at 562 nm. Cell treatment conditions were performed in replicates of three to five. Error bars denote the standard deviation of the mean MTT activity, as indicated in Figure 1C–D.

Sample Preparation for MS Analysis—Sample preparation of OVCAR3 cell pellets and conditioned media was performed as previously described by our group (26, 27). Cells were plated on 10 cm^2 plastic dishes and treated as described above. For each condition, two dishes containing 1$\times$ 10^6 cells per dish were seeded per treatment condition and per time point. Following the treatment regimen, cells were pooled for each treatment group at each time point and were sonicated. Conditioned media was concentrated via centrifugation using CentriPrep units (Millipore, Billerica, MA). Total protein concentrations were determined via BCA protein analysis (Thermo Scientific). 150 μg protein lysates were reduced in 12 mM Tris (2-carboxyethyl) phosphine and 0.1% SDS for 60 min at 60 °C, alkylated with 50 mM iodoacetamide for 30 min, and digested overnight with sequence grade trypsin at 37 °C. SDS-PAGE and silver staining analyses were performed to ensure complete tryptic digestion. Peptides were desalted on Sep-Pak C18 columns (Waters Corporation, Milford, MA) and vacuum dried.

iTRAQ Labeling of Peptides—Desalted tryptic peptides were labeled with isobaric tags for relative quantification using iTRAQ 8-plex reagents (AB Sciex, Foster City, CA) per the manufacturer's instructions and as described elsewhere (28). Briefly, peptides were dried and resuspended in 20 μl iTRAQ dissolution buffer. Each iTRAQ 8-plex reagent was dissolved in 60 μl isopropanol, vortexed, and added to each specimen. Isobaric tags with *m/z* of 113, 114, 115, 116, 117, 118, 119, and 121 were added as follows: control-treated OVCAR3 lysates, LY294002-treated lysates, EGF-treated lysates, combinatorial EGF and LY294002-treated lysates, control-treated conditioned media, LY294002-treated media, EGF-treated media, and combinatorial EGF and LY294002-treated media, respectively. Three iTRAQ 8-plex labeling schemes were performed on specimens treated for 12, 24, and 48 h. Each mixture was incubated at room temperature for 2 h, labeled peptides were combined per time point, and specimens were desalted as previously described (28).

LC-MS/MS Analysis—iTRAQ-labeled tryptic peptides were analyzed via LC-MS/MS using an LTQ-OrbitrapVelos (Thermo Fisher, Waltham, MA). Strong cation exchange fractionation was performed on a house-packed 300 μm Polysulfoethyl A (PolyLC) column at a rate of 5 μl/min. Per 8-plex-labeled iTRAQ set, which corresponds to 12-, 24-, and 48-h treatment groups, nine fractions were collected, with the first and last fractions being pooled, yielding eight fractions per time point. Each fraction was desalted on a Waters Oasis hydrophilic-lipophilic balance micro-elution plate and subsequently injected into the mass spectrometer using an Agilent autosampler coupled to an Eksigent 2D Nano LC system. Peptides were trapped at a rate of 5 μl/min onto a 2.5-cm trap column and eluted onto a Magic C18 column (5-μm particles with 100-Å pore size). Chromatographic separation was performed at 300 nl/min with a 90-min gradient from 95% A/5% B to 68% A/32% B (A = water containing 0.1% formic acid, B = 90% acetonitrile containing 0.1% formic acid) into an Orbitrap Velos operating in high-energy collision-induced dissociation mode with the normalized collision energy set to 45.

Data Analysis for Peptide Identification and Quantitation—Raw MS/MS analysis of iTRAQ-labeled peptides was searched with MASCOT (version 2.2.0) using Proteome Discoverer version 1.3.0.339 (Thermo Fisher) against the NCBI human reference sequence database (Refseq 40 Complete, released on April 16, 2010, with 29,704 entries). Precursor and fragment mass tolerance were set at 10 ppm and 0.05 Da, respectively. Database-searching parameters included the following: static modifications for carbamidomethyl (C) and iTRAQ 8plex (N-term), and dynamic/flexible modifications for oxidation (M), iTRAQ8plex (K), and iTRAQ8plex (Y). For protein identification using the Proteome Discoverer software, the following selection filters were applied: a 5% false discovery rate, a MASCOT significance cutoff of 0.1052, a medium peptide confidence score, and a peptide rank of 1.

Quantitation of iTRAQ-labeled peptides was achieved using the LTQ-Orbitrap and Proteome Discoverer software. Data were searched from the .RAW data files and searched again with the Xtract module before the results were combined. Data normalization was achieved via the summation of all peptide signals for each treatment group (vehicle, EGF, LY294002, and combinatorial EGF and LY294002) for both cellular lysate samples, as well as for conditioned media. To determine the normalized peptide intensity, for each peptide, the signal intensity was divided by the standardized summation for the respective treatment group. Further, protein signal normalization was achieved via averaging of the relative intensities of all peptides identified for each protein. These ratios provide a relative expression of growth-stimulated or -inhibited proteins over time. The level of proteins exceeding a 1.5-fold change (p value $<$ 0.05) was classified as significantly up- or down-regulated relative to vehicle-treated lysates. Statistically, the p value was designated as the calculation of the probability of a protein change exceeding what would be observed under a normal Gaussian distribution (null hypothesis). A

logarithmic transformation was performed on all proteins, assuming a Gaussian distribution, to determine the means and standard deviations from all protein data; a fold change of ±1.5 corresponds to a p value < 0.05. The data associated with this manuscript are available for download at the Proteome Commons Tranche using the following hash: JKfKGUfOV1ac5d5ysSokBvLv3ZHf+SUVb/UWqHxM2ZD8sD/8A3Kn/Fo31vr6bIedWgoy5rVr3Ge9wh1vxkd3YB9qXeMAAAAAAAALvA==.

Pathway Analysis—The Ingenuity Pathway Analysis module (Ingenuity® Systems) was applied to all EGF-regulated proteins at 12, 24, and 48 h treatment to identify signaling pathways associated with EGF stimulation. Proteins associated with canonical pathways were deemed significant using Fisher's exact test (p value < 0.01) to determine the probability that the association between identified proteins and a canonical pathway could be explained by chance alone.

Immunohistochemical Analysis—Normal human ovarian tissue and human ovarian tumor tissue sections (4 μm, paraffin-embedded, ProSci, Poway, CA) or normal or human fallopian tube adenocarcinoma tissue sections (4 μm, paraffin-embedded, Origene Technologies, Rockville, MD) were deparaffinized through a series of xylene washes to PBS, and immunohistochemical analysis was performed using the EnVision+ System-HRP 3,3′-diaminobenzidine (DAB) kit (Dako, Carpinera, CA) according to the manufacturer's specifications. Briefly, sections were incubated with 0.03% hydrogen peroxide and incubated with primary antibodies diluted in PBS containing 0.1% Tween-20 and 5% BSA for 90 min at room temperature in a humidified chamber or overnight at 4 °C. Primary antibodies included affinity purified mouse monoclonal anti-LAMP-1, clone E-5 (2 μg/ml, Santa Cruz Biotechnologies, Santa Cruz, CA), or mouse IgG immunoglobulin (1 μg/ml, Dako) as a control. HRP-conjugated secondary antibody and DAB precipitation was performed using the EnVision+ System-HRP per the manufacturer's instructions. Sections were counterstained with hematoxylin for contrast. Tissue sections were examined for staining intensity and immunoreactivity, and images were captured on a pathological digital scanner (ScanScope, Aperio Technologies, Vista, CA) using ImageScope viewing software (v11.1.2.760, Aperio Technologies, Vista, CA).

Tissue microarray (TMA) analysis was performed on 100 cores from 100 cases (1 core per case) of ovarian adenocarcinoma of various stages and grades, including the following: 5 cases of ovary clear cell carcinoma, 62 ovary serous papillary adenocarcinoma, 10 ovary mucinous papillary adenocarcinoma, 2 ovary endometrioid carcinoma, 1 ovary metastatic adenocarcinoma, and 10 ovary metastatic serous papillary adenocarcinoma. In addition, six normal ovary tissues and four tumor-adjacent normal ovary tissues were included in the analysis. Paraffin-embedded cores were 5 μm in thickness, and TMA sections were obtained from US Biomax (Rockville, MD, catalogue number BC11115). Immunohistochemical analysis was performed as previously described. Primary antibodies included rabbit monoclonal anti-EGF Receptor (XP) (1:750, Cell Signaling, Boston, MA), mouse anti-LAMP-1, and rabbit anti-aconitase 2. Staining pattern and intensity were scored by a pathologist at Johns Hopkins Medical Institutions. All the pathological information including tumor grade, stage and histological type of the TMA cases was provided by the company (US Biomax).

RESULTS

EGF Modulates OVCAR3 Proliferation—In order to assess ovarian cancer cell proliferation, the human serous ovarian adenocarcinoma cell line OVCAR3 was treated with pro- and/or anti-proliferative stimuli. OVCAR3 cells were treated with EGF (50 ng/ml) and/or the PI3K/Akt inhibitor LY294002 (25 μM) for 12 to 48 h. Upon EGF treatment, the induction of pAkt was observed 12 h post-treatment, and levels of the phosphorylated form of Akt were potentiated 48 h post-EGF exposure. Further, the induction of EGF-stimulated pAkt in OVCAR3 cells was abolished via co-administration with LY294002, a PI3K inhibitor (Figs. 1*A*, 1*B*).

Cell proliferation studies were conducted to assess the kinetics of EGF treatment in OVCAR3 cell growth. Cellular proliferation was determined via MTT cleavage by cellular mitochondrial dehydrogenases. Although there was no statistically significant increase in cellular proliferation 12 h post-EGF treatment, there was a 1.9-fold increase in cellular growth 48 h post-EGF stimulation relative to control-treated cells (Figs. 1*C*, 1*D*). However, 48 h post-treatment with LY294002 alone or in combination with EGF, there were 2.0- and 1.9-fold decreases in cell growth relative to control-treated samples, respectively. These data illustrate that the increased proliferation observed with EGF treatment occurs downstream of the molecular activation of the PI3K/Akt pathway, and EGF stimulation results in Akt activation prior to the observation of increased cellular growth.

Quantitative Analysis of Proteins in Growth-stimulated Ovarian Cancer Cells—In order to identify proteins expressed in stimulated OVCAR3 cells over time, quantitative proteomic analysis was performed on both cellular lysates and the conditioned media of growth-stimulated or inhibited cells. As EGF stimulation results in Akt pathway activation prior to increased proliferation, cells were vehicle-treated or dosed with EGF, LY294002, or a combination, for 12, 24, or 48 h. Proteins collected from cell lysates and conditioned media from treated OVCAR3 cells were trypsin digested. Tryptic peptides for each time point were 8-plex iTRAQ labeled and combined prior to MS analysis. For each time point, specimens were separated on a micro-SCX column into eight separate fractions, and each fraction was analyzed using LC-MS/MS. From the 12, 24, and 48 h time points, 1242, 1226, and 1110 proteins were identified, respectively (supplemental Tables S1–S3).

Candidate Selection for Proteins Regulated by EGF—In order to identify the proteins regulated by EGF, EGF-treated cellular lysates were analyzed to assess differentially regulated proteins as compared with vehicle-treated specimens. The protein abundance in EGF-treated cells relative to that in vehicle-treated lysates was calculated for each time point. Proteins that exhibited a greater than 1.5-fold change (p value < 0.05) were demarcated as regulated by EGF. For the 12, 24, and 48 h time points, 98, 135, and 104 regulated proteins were identified, respectively (supplemental Tables S4–S6), with 39 proteins regulated at multiple time points post-EGF exposure (Fig. 2*A* and Table I). Subcellular distribution analysis of EGF-regulated proteins revealed that the majority of commonly identified proteins were cytoplasmic proteins (57%), and roughly one quarter (24%) of proteins were nuclear proteins (Fig. 2*B*). Very few proteins associated with

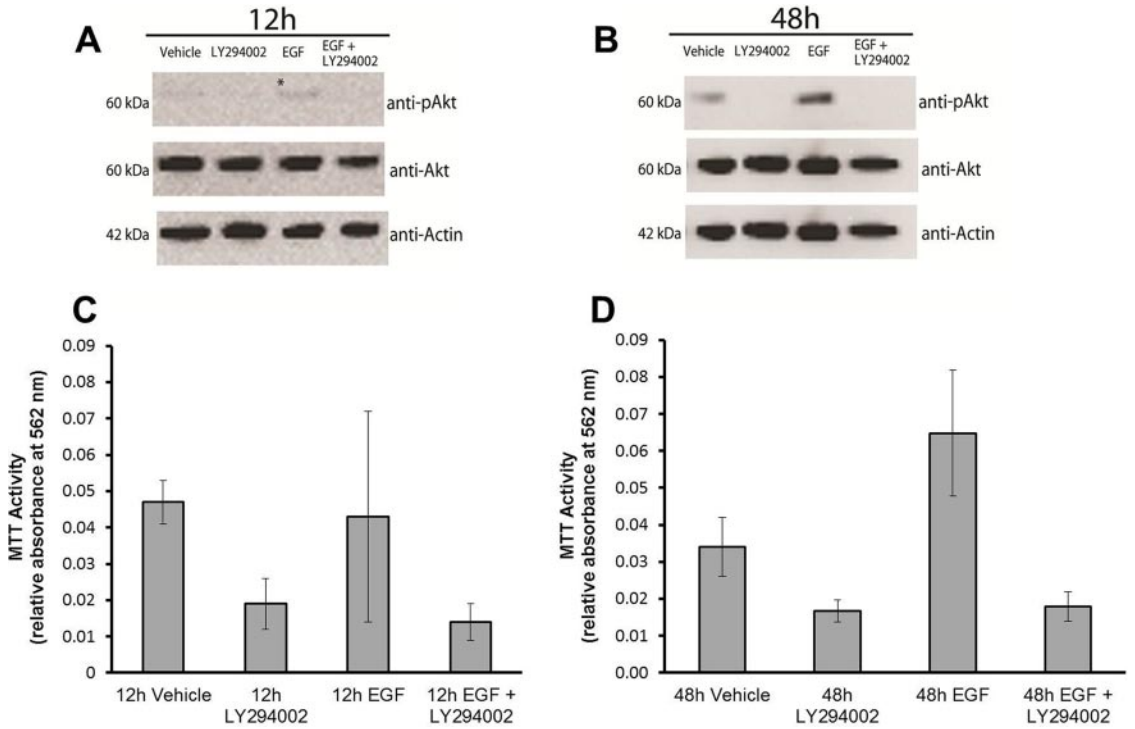

FIG. 1. **OVCAR3 regulation by EGF and LY294002.** *A*, *B*, Akt activation (phosphorylated Akt, pAkt) in OVCAR3 cells at 12 and 48 h post-treatment. The pAkt level is increased in the presence of EGF at 12 h (*) and 48 h and reduced in the presence of PI3K inhibitor, LY294002. Protein levels were normalized to an actin (42 kDa) loading control. *C*, *D*, MTT proliferation assay of OVCAR3 cells at 12 and 48 h post-treatment. Formazan formation (absorbance at 562 nm) was used to determine the cell proliferation.

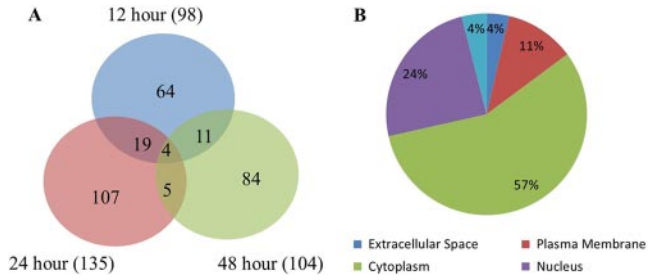

FIG. 2. **OVCAR3 proteomics analysis using iTRAQ labeling and tandem mass spectrometry.** *A*, EGF stimulation resulted in the identification of 98, 135, and 104 significantly regulated proteins at 12, 24, and 48 h post-exposure, respectively (p value < 0.05). *B*, subcellular distribution of all proteins significantly altered following EGF treatment ($n = 294$ proteins across 48 h time course).

the plasma membrane (11%) or the extracellular space (4%) were identified with changes following EGF treatment.

Subsequent pathway analysis of EGF-regulated pathways indicated a significant association with several cellular signaling cascades (Table II). Regulated proteins are associated not only with the expected EGF signaling, ERK/MAPK signaling, and PI3K/MAPK pathways, but also with cascades involved in mTOR signaling, cell cycle regulation, and actin cytoskeletal dynamics. A full pathway analysis, including the identities of temporally associated molecules, is included in supplemental Table S7.

Of the identified EGF-responsive candidates, several proteins were observed over time. The selection of a candidate for further validation studies was based on several criteria. Selection criteria included (a) the temporal pattern of protein stimulation or inhibition with EGF exposure, (b) the protein regulatory pattern in the presence of the PI3K inhibitor, and (c) the potential biological relevance of the molecule in cancer progression, which was determined through literature review. Based on these criteria, subsequent studies were focused on LAMP-1. According to quantitative analysis of LAMP-1 abundance in OVCAR3 cells, LAMP-1 is significantly and specifically up-regulated 24 h post-EGF treatment (normalized ratio, 1.84) but significantly down-regulated 48 h post-EGF exposure (normalized ratio, 0.41) relative to vehicle-treated cells (Table I). LAMP-1 abundance was determined as the ratio of the protein in the presence of anti- or pro-growth stimuli to the protein level present under vehicle conditions (Fig. 3). These data were normalized to the vehicle cell lysate treatment condition at each collection point. Treatment with the PI3K inhibitor had no impact on LAMP-1 protein abundance (1.20 and 0.91 at 24 and 48 h post-treatment, respectively) (supplemental Tables S5, S6). However, the co-administration of EGF and LY294002 to OVCAR3 cells illustrated that EGF-stimulated expression of LAMP-1 24 h post-treatment was not inhibited by the PI3K inhibitor (normalized ratio, 1.51), but protein expression was down-regulated 48 h post-exposure

TABLE I

Significantly changed proteins post–EGF exposure; proteins identified with significant changes following EGF treatment at at least two time points over a 12 to 48 h time course, $p < 0.05$

Accession number	Protein name	12 h EGF	24 h EGF	48 h EGF
117553627	Acetylserotonin O-methyltransferase-like	1.62	3.15	1.62
210147571	Acidic (leucine-rich) nuclear phosphoprotein 32 family, member E	0.57	0.45	N/A
4501867	Aconitase 2, mitochondrial	N/A	0.37	0.58
24308338	Actin filament associated protein 1-like 2	0.54	0.56	N/A
4557251	ADAM metallopeptidase domain 10	1.76	N/A	2.19
4502227	ADP-ribosylation factor-like 1	0.66	0.65	N/A
4506797	Ataxin 7	0.63	0.66	N/A
41281429	Basic leucine zipper and W2 domains 1 pseudogene 1; basic leucine zipper and W2 domains 1 like 1; basic leucine zipper and W2 domains 1	2.28	3.80	N/A
51599156	Chromodomain helicase DNA binding protein 4	1.60	1.71	N/A
41281603	Chromosome 19 open reading frame 33	0.48	0.26	N/A
221316630	Coatomer protein complex, subunit beta 1	1.85	1.52	N/A
21070976	Diablo homolog	N/A	1.54	1.50
6912328	Dimethylargininedimethylaminohydrolase 1	3.59	N/A	6.02
24430135	Dolichyl-phosphate mannosyltransferase polypeptide 3	1.52	N/A	1.52
18426915	Drebrin 1	1.77	N/A	1.83
166362728	Epidermal growth factor	1.71	N/A	2.65
5031711	Eukaryotic translation initiation factor 1B	1.52	1.61	N/A
151108473	Fission 1 (mitochondrial outer membrane) homolog	N/A	0.59	1.54
17149836	FK506 binding protein 1A, 12 kDa	1.72	2.41	N/A
194018522	G1 to S phase transition 1	1.51	1.61	N/A
4758442	Glia maturation factor, beta	0.62	2.04	N/A
20127446	Integrin, beta 5	2.08	0.48	N/A
112380628	Lysosomal-associated membrane protein 1	N/A	1.84	0.41
4504957	Lysosomal-associated membrane protein 2	0.65	N/A	0.44
54873600	Mesencephalic astrocyte-derived neurotrophic factor	2.73	N/A	0.46
32483374	NOP56 ribonucleoprotein homolog	2.16	1.71	2.57
7706254	NOP58 ribonucleoprotein homolog	1.90	1.82	1.71
56118310	Nuclear casein kinase and cyclin-dependent kinase substrate 1	0.64	0.62	N/A
7662018	PHD finger protein 3	3.24	2.49	N/A
21735598	Programmed cell death 4 (neoplastic transformation inhibitor)	0.64	N/A	0.56
124494254	Proliferation-associated 2G4, 38 kDa; proliferation-associated 2G4 pseudogene 4	1.88	N/A	1.67
13376751	Proteasomal ATPase-associated factor 1	1.68	N/A	1.70
44680114	Proteasome (prosome, macropain) assembly chaperone 1	1.58	1.80	N/A
94429050	SEC22 vesicle trafficking protein homolog B	1.56	1.73	N/A
115583685	Solute carrier family 16, member 1 (monocarboxylic acid transporter 1)	2.09	2.10	2.09
25777713	S-phase kinase-associated protein 1	1.80	1.89	N/A
224493972	Thioredoxin domain containing 5 (endoplasmic reticulum); muted homolog	1.63	1.82	N/A
218931148	Tropomodulin 2 (neuronal)	0.53	N/A	0.52
34098946	Y box binding protein 1	N/A	2.09	0.66

(normalized ratio, 0.50), similar to observations after EGF treatment alone (supplemental Tables S5, S6). These data suggest that although LAMP-1 is regulated by EGF in a temporal manner, the expression of LAMP-1 occurs independently of the PI3K/Akt signaling cascade. Of proteins with significantly altered expression levels post-EGF treatment, only one other candidate exhibited a trend similar to that of LAMP-1. Y box binding protein 1 also showed differential

TABLE II
Ingenuity Pathway Analysis of EGF-treated OVCAR3 cells; subset of proteins and subsequent canonical pathways associated with EGF treatment of OVCAR3 cells ($p < 0.01$)

Ingenuity canonical pathways	−log (*p* value)	Ratio	Molecules
EIF2 signaling	6.49	8.2×10^{-2}	RPS28, EIF3E, EIF3C/EIF3CL, EIF2A, RPL37, RPL36, RPS27, RPS13, RPS9, EIF5, EIF3I, MAP2K1, RPL18, EIF3L, RPS14
mTOR signaling	4.26	6.52×10^{-2}	RPS27, PRKCI, RPS13, PPP2CA, RPS28, RPS9, EIF3I, FKBP1A, EIF3E, EIF3C/EIF3CL, EIF3L, RPS14
Integrin signaling	1.3	3.41×10^{-2}	ARF1, ARPC5, ZYX, TLN1, ITGA3, MAP2K1, ITGB5
Regulation of actin-based motility by Rho	1.28	4.65×10^{-2}	PFN1, ARPC5, PFN2, ARHGDIA
FAK signaling	1.22	4.08×10^{-2}	EGF (includes EG:13645), TLN1, ITGA3, MAP2K1
Ephrin receptor signaling	1.13	3.09×10^{-2}	GNB1, ARPC5, ADAM10, EGF (includes EG:13645), ITGA3, MAP2K1
ERK/MAPK signaling	1.01	3.03×10^{-2}	PRKCI, PPP2CA, TLN1, ITGA3, MAP2K1, HSPB1
Rac signaling	9.96×10^{-1}	3.42×10^{-2}	PRKCI, ARPC5, ITGA3, MAP2K1
PI3K/AKT signaling	8.68×10^{-1}	3.1×10^{-2}	CDC37, PPP2CA, ITGA3, MAP2K1
Actin cytoskeleton signaling	8.5×10^{-1}	2.67×10^{-2}	PFN1, ARPC5, PFN2, EGF (includes EG:13645), ITGA3, MAP2K1
Cyclins and cell cycle regulation	8.37×10^{-1}	3.45×10^{-2}	PA2G4, PPP2CA, LOC728622/SKP1
EGF signaling	7.3×10^{-1}	4.17×10^{-2}	EGF (includes EG:13645), MAP2K1
Cell cycle: G1/S checkpoint regulation	6.26×10^{-1}	3.39×10^{-2}	PA2G4, LOC728622/SKP1
Mitotic roles of polo-like kinase	5.82×10^{-1}	3.33×10^{-2}	PPP2CA, SMC1A
Death receptor signaling	5.82×10^{-1}	3.23×10^{-2}	DIABLO, HSPB1
Tight junction signaling	5.78×10^{-1}	2.55×10^{-2}	PRKCI, PPP2CA, VAPA, CTNNA1
Cell cycle control of chromosomal replication	4.28×10^{-1}	3.33×10^{-2}	MCM7
Cell cycle: G2/M DNA damage checkpoint regulation	2.8×10^{-1}	2.08×10^{-2}	LOC728622/SKP1

up-regulation 24 h post-EGF treatment (normalized ratio, 2.09), with decreased protein levels 48 h post-exposure (normalized ratio, 0.66). However, because of its potential implications in cancer progression, LAMP-1 was further validated using downstream antibody-based approaches.

Candidate Verification via Antibody-based Studies—Based on findings from proteomic analysis of the EGF-stimulated OVCAR3 cell system, it was hypothesized that regulation of LAMP-1 occurs in the early stages of cellular proliferation. To determine whether these findings could be translated to the differential expression of LAMP-1 prior to tumor metastasis, immunoblotting was performed on tissue lysates of serous adenocarcinomas of varying stages. Commercial lysates from normal ovarian tissue, as well as from serous adenocarcinomas that were FIGO stages IIb and III and ovarian adenocarcinoma FIGO stage IV (liver metastasis), were acquired, and equal microgram amounts of protein were analyzed for relative LAMP-1 protein levels. These initial studies demonstrated a notable relative increase in LAMP-1 protein levels in stages IIb and III tumor lysates compared to normal ovarian tissue, and a marked decrease in ovarian adenocarcinoma tissue that metastasized to the liver (Fig. 4*A*).

The immunoblotting findings were also recapitulated via immunohistochemistry. LAMP-1 exhibited specific staining in ovarian cancer tissue sections, with strong staining in the epithelial cell cytoplasm. No staining was observed in normal tissue sections or control sections probed with mouse immunoglobulin (Figs. 4*B*–4*K*). Further, Western blotting analysis was performed using antibodies targeted against aconitase 2 (NCBI accession no. 4501867). Although aconitase 2 protein levels were decreased following EGF treatment (Table I), neither protein fit the aforementioned selection criteria for full validation. Unlike the regulation observed in ovarian tissue lysates of varying stages, aconitase 2 was not differentially expressed across tumor lysate stages (data not shown).

Of note, recent studies have suggested that serous ovarian cancers arise from the fallopian tube via unrestrained PI3K activity (29, 30). Consequently, LAMP-1 expression in normal fallopian tissue and serous papillary fallopian adenocarcinoma was assessed (supplemental Fig. S1). Very weak stain-

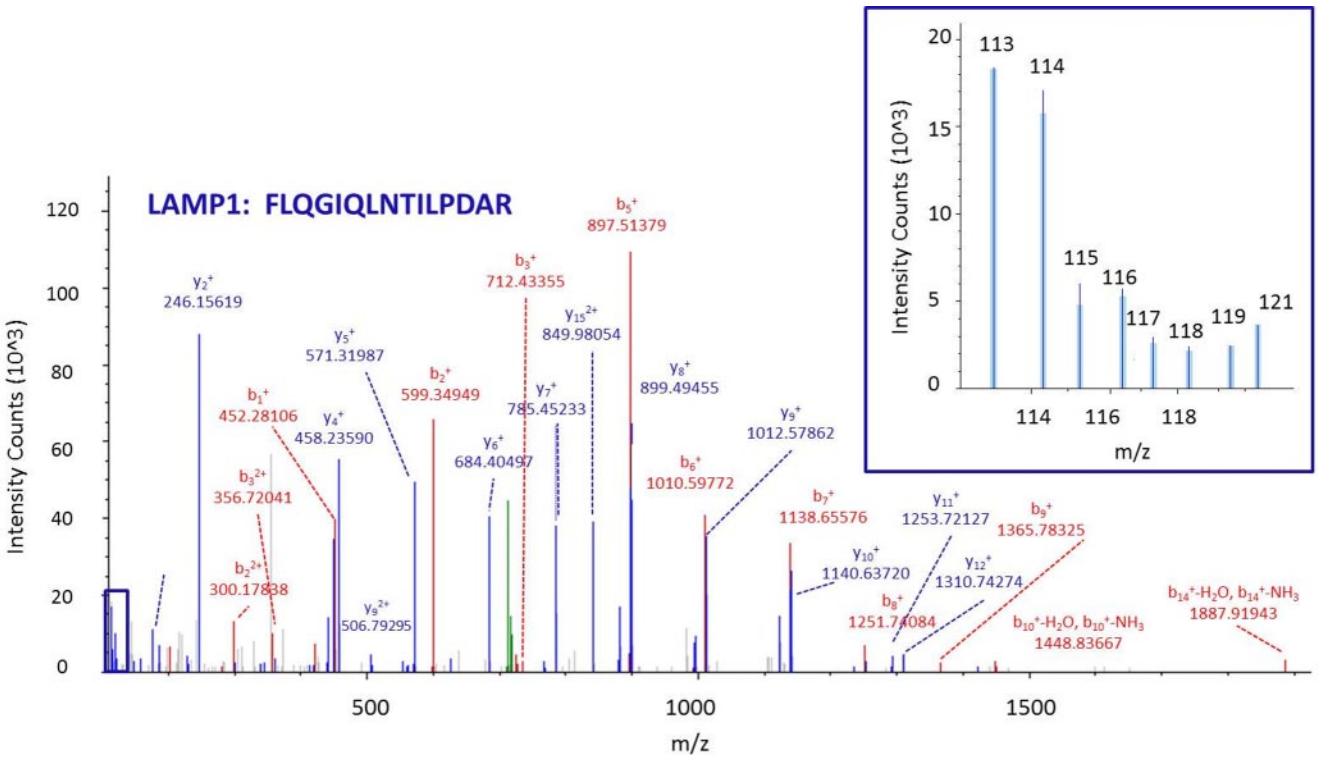

FIG. 3. **MS/MS spectrum of a LAMP-1 peptide.** MS/MS spectrum of the identified peptide (FLQGIQLNTILPDAR) corresponding to the protein LAMP-1 from ovarian OVCAR3 cells treated with anti- or pro-growth stimuli for 48 h. The peptides were labeled with 8-plex iTRAQ reagents and analyzed via LTQ-Orbitrap. The inset shows the relative abundances of iTRAQ isobaric mass labels.

ing was observed in the cytoplasm of fallopian stromal cells. However, much like the aforementioned observations in serous epithelial ovarian adenocarcinoma cells, LAMP-1 was highly expressed throughout fallopian adenocarcinoma tissue sections, particularly in the epithelial cytoplasm. These data suggest a potential role of LAMP-1 in identifying other forms of gynecological malignancies, including those originating in the fallopian tube.

In order to assess a large pool of specimens, TMA analysis was performed on 100 cores containing normal and pathogenic ovarian cases. Although the majority of cores were serous papillary adenocarcinomas of varying FIGO stages, lymph node metastatic, mucinous adenocarcinoma, endometrioid adenocarcinoma, and normal ovarian cancer cases were also represented. LAMP-1 expression was observed in a subset of serous adenocarcinoma tissue sections (22/62, 35%; Table III). In stained serous ovarian malignant sections, LAMP-1 expression was found in the epithelial cytoplasmic structures. In scoring for intensity, 29% of serous adenocarcinoma sections exhibited weak staining (a score of 1), whereas only four serous adenocarcinoma cores were scored as moderately stained (a score of 2). Fig. 5 illustrates serous ovarian adenocarcinoma sections that exhibited no (Figs. 5*A*, 5*B*), weak (Figs. 5*C*, 5*D*), or moderate (Figs. 5*E*, 5*F*) epithelial staining. In addition, 3 of 10 metastatic tumor sections showed LAMP-1 expression; however, one core exhibited specific staining in stromal cell populations, and the other two specimens stained weakly for LAMP-1. Tissue microarray analysis also revealed that of the serous adenocarcinomas exhibiting LAMP-1 expression, the majority were from grade 2 ovarian carcinoma (8 of 14; 57%), and approximately half of analyzed serous malignant adenocarcinoma cores also showed weak LAMP-1 staining at various disease stages, with the exception of stage III and IIIc tumors (Table III, supplemental Table S8, and supplemental Fig. S2). It should also be noted that only one normal tissue core expressed LAMP-1 (signal was observed in a small cluster of germinal cells), and all other non-cancerous tissue exhibited undetectable LAMP-1 expression (data not shown).

Tissue analysis was also performed using antibodies targeted to the EGF receptor and aconitase 2. Aconitase 2 was expressed at moderate to high levels in nearly all analyzed ovarian cores (96/100), including in the stromal cells of normal ovarian tissue (supplemental Table S8 and data not shown). These findings further illustrate a lack of regulation across ovarian tissue stages and are consistent with previous Western blotting findings. Of note, comparable tissue cores probed with EGFR illustrate that 16 of 22 (73%) LAMP-1 positive serous adenocarcinoma cores also stained positive for EGFR (Table III and supplemental Table S8). Additionally, 15 of 18 (83%) LAMP-1 positive FIGO stage I/II

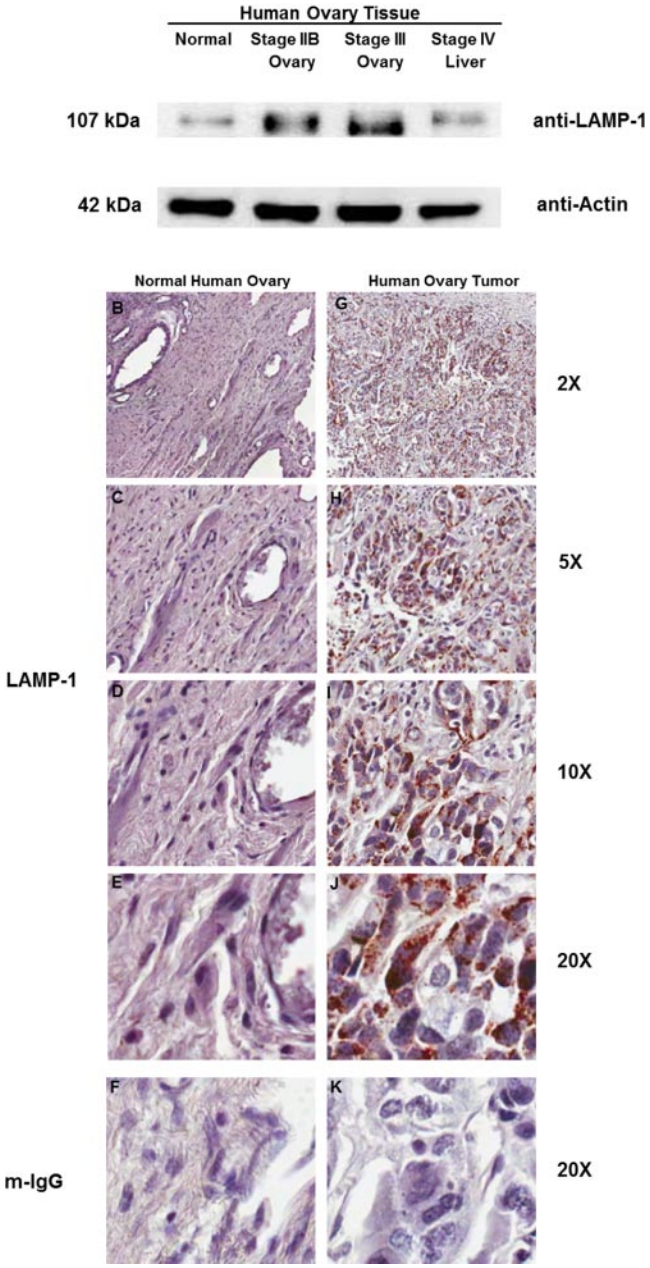

FIG. 4. **LAMP-1 antibody-based studies.** *A*, Western blot analysis of normal and stage-specific tissue lysates. LAMP-1 is detected at ~110 kDa. 10 μg total protein lysates loaded. Protein levels were normalized to actin loading control. Aconitase 2 is detected at ~80 kDa. Protein levels were normalized to tubulin loading control. *B–K*, immunohistochemical analysis of normal and cancerous ovarian tissue. LAMP-1 is not stained in normal ovarian tissue sections (*B–E*). Sections stained with mouse IgG as a negative control. LAMP-1 is expressed in serous epithelial ovarian adenocarcinoma tissue sections (*G–J*). LAMP-1 expression is specifically observed in the cytoplasm of epithelial cells. Absence of the LAMP-1 specific staining when probed with mouse immunoglobulin as a negative control (*K*).

cores exhibited moderate to strong EGFR signal. These data further support a potential relationship between aberrant EGFR expression and increased LAMP-1 protein expression.

DISCUSSION

This study focuses on the temporal differences within a serous adenocarcinoma cell line. Proteomic studies of iTRAQ-labeled peptides identified several candidates differentially expressed over time in EGF growth-stimulated cells relative to control OVCAR3 cells. Further, canonical pathway analysis of altered proteins from treated OVCAR3 cells identified several proteins associated with EGF-stimulated cascades, including the mTOR signaling and RhoA signaling pathways, as well as actin cytoskeletal regulation (31–33). LAMP-1 was selected and studied more closely using antibody-based approaches in ovarian cancer tissues.

Although the ovarian carcinoma biomarker CA-125 is utilized in monitoring the response of patients to therapy, it is not ideal for identifying ovarian tumors in the early stages of the disease, nor is it effective in predicting therapeutic outcomes. Thus, we used a quantitative MS approach to identify potential ovarian tissue tumor markers using a homogeneous cell population of growth-manipulated ovarian cells. Because of their cellular homogeneity and ease of use, many studies have utilized human ovarian cancer lines for proteomics discovery. Such studies include comparisons of proteomic profiles between low- and high-grade serous epithelial cell lines (34); comparisons of lysate, membrane-associated, and secreted proteins between immortalized cell lines and primary ascites (21); global comparisons of secretomes across different epithelial ovarian cancer subtypes (20); and the identification of biomarkers associated with chemotherapeutic resistance in ovarian cancers (27).

Epithelial ovarian tumors are both morphologically and biologically heterogeneous; thus, the identification of tissue biomarkers in a homogeneous population of tumor cells proves difficult. By using the ovarian serous adenocarcinoma OVCAR3 cell line as a model, we were able to stimulate molecular signaling cascades observed during cancer progression in order to ultimately identify candidate proteins associated with hyperproliferative growth dynamics in a homogeneous cellular population. The OVCAR3 cell line was used as a model because of the molecular and morphological similarities observed between the cells and malignant epithelial ovarian tumors (24). Because the OVCAR3 cell line is an immortalized cancer cell line, it is not currently being used as a surrogate to identify proteins to discriminate between cancer and non-cancer; rather, the utility of the system has been focused on identifying differentially expressed proteins as a population of cancer cells hyperproliferates. A single cell line was pursued in this work to illustrate changes in protein levels over time from a homogeneous cell population. Based on the findings from this analysis, current studies are focused on

TABLE III
LAMP-1 tissue microarray

Tissue characteristic	LAMP-1 positive, *n* (%)	EGFR positive, *n* (%)	LAMP-1 positive also positive for EGFR, *n* (%)
Serous	22 (35)	45 (74)	16 (73)
Grade			
1	4 (31)	11 (85)	3 (75)
2	8 (57)	11 (79)	6 (75)
3	10 (31)	21 (66)	7 (70)
FIGO stage			
I/II	18 (41)	34 (77)	15 (83)
III	2 (13)	10 (67)	0 (0)
IV	2 (67)	1 (33)	1 (50)
Mucinous	2 (22)	4 (44)	1 (50)
Clear cell	1 (20)	5 (100)	1 (100)
Endometrioid	0 (0)	0 (0)	0 (0)
Metastatic serous	3 (30)	5 (50)	1 (33)
Normal tissue	1 (17) (germinal)	1 (17) (stromal)	0 (0)
Normal adjacent tissue	0 (0)	0 (0)	0 (0)

100 ovarian cores scored for LAMP-1 and EGFR expression. Scoring based on protein expression. 0 = no staining; 1 = weak staining; 2 = moderate staining; 3 = strong staining. Further classification of TMA can be found in supplementary Table S8.

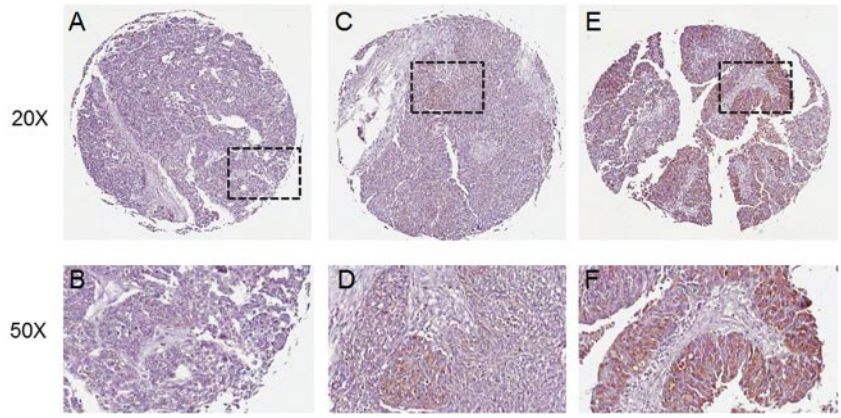

FIG. 5. **LAMP-1 expression in ovarian carcinoma tissue cores.** TMA cores for malignant serous adenocarcinoma sections showing no staining (*A* and *B*), weak staining (*C* and *D*), and moderate cytoplasmic epithelial staining (*E* and *F*). Sections are counterstained with hematoxylin.

identifying differentially expressed proteins in primary ovarian tissues in different stages.

Increased cellular proliferation and motility are crucial prerequisites for the invasion of malignant tumors into surrounding tissues and the formation of metastases *in vivo* (35). Thus, there is a distinction between the detection of a cancerous cell *in situ* and the conditions required for metastatic formation at distant sites. If focus is placed on the molecular events that occur during the initiation of cancer cell hyperproliferation, biomarkers can be identified to aid in ovarian cancer prognosis, as well as to serve as potential predictors of treatment regimens. To drive increased cellular proliferation in OVCAR3 cells in this study, the PI3K/Akt/mTOR pathway was stimulated with EGF. EGF is a ligand of the EGFR, facilitating receptor dimerization and tyrosine kinase activation, and can stimulate several downstream signaling cascades associated with cellular proliferation and survival, including the PI3K/Akt/mTOR pathway (17, 36). Conversely, LY294002 is a flavonoid derivative and is a potent inhibitor of the P13K/Akt/mTOR signaling cascade, eliciting its effect through competitive, reversible binding to the ATP binding site of PI3K (24, 37). In addition, EGFR activation stimulates several other PI3K/Akt/mTOR-independent signaling cascades that regulate cell growth, angiogenesis, and tumor metastasis (17, 38, 39).

LAMP-1, also known as CD107a, is a highly N- and O-linked glycosylated molecule expressed in endosomes and lysosomal substructures of cells (40–42). Although primarily expressed within the cells in the aforementioned organelles, a small percentage of LAMP-1 also localizes to the plasma membrane (43–45). Proper transport of LAMP-1 from the *trans*-Golgi network to the lysosomes requires a tyrosine motif in the cytoplasmic tail of the protein; disruption of this motif results in LAMP-1 expression at the cell surface (46). Increased LAMP-1 expression at the cell surface has been observed during platelet and granulocytic cell activation, as well as in metastatic tumor cells (42, 47, 48). LAMP-1 has also been implicated in cancer progression and tumor metastasis. Studies of lung endothelial cells have suggested that one manner in which LAMP-1 might facilitate metastasis is via increased translocation to the cell membrane, where it acts as

a ligand to galectin-3 (49, 50). However, correlation studies performed in patients with pancreatic carcinomas suggest that increased levels of LAMP-1 exhibit improved outcomes post-tumor resection (51). Thus, the exact mechanisms through which LAMP-1 might play a role in cancer cascades are not completely understood.

The tissue microarray analysis for LAMP-1 demonstrated positive protein staining in roughly one-third (35%) of ovarian serous adenocarcinoma cores. However, the protein was not expressed in all malignant ovarian tissues. Further TMA analysis for EGFR illustrated that 69% of LAMP-1 positive cores also stained positive for EGFR. Additionally, the relationship between EGFR overexpression and LAMP-1 levels is supported by gene set enrichment analysis, which assessed the potential significance of LAMP-1 in the EGFR pathway using the Cancer Genome Atlas (TCGA). TCGA contains 589 patients with microarray gene expression, and 31 genes were identified as being involved in the EGF pathway. Gene-set enrichment analysis (GSEA) was performed to assess the association of LAMP-1 in EGFR-mediated signaling cascades. GSEA analysis revealed that LAMP-1 is positively associated with EGFR-modulated molecular pathways (p value < 0.0060). The genomic analysis is consistent with our proteomics data and validation studies, which demonstrate a significant positive correlation between LAMP-1 and EGF treatment. The observation that not all EGFR-positive cores exhibited LAMP-1 immunoreactivity might be due to EGFR-induced dysregulation of other signaling cascades. Although we have demonstrated a modest correlation between EGFR and LAMP-1 expression in ovarian cancer tissue cores, it is important to note that increased expression of EGFR is not always predictive of therapeutic responses to receptor-targeted therapies. This has been demonstrated in both ovarian and colorectal cancers (12, 52). Clinical trials performed using an EGFR monoclonal antibody for the treatment of receptor-positive cancers did not demonstrate clinical efficacy as a monoclonal antibody therapy, further illustrating the difficulty of predicting antibody responses based on overexpression alone (53). However, the positive LAMP-1 signal might be predictive of a specific ovarian cancer modality and might assist in treatment in EGFR-positive serous ovarian malignancies.

Recently, studies demonstrated *Lamp-1* mRNA up-regulation in OV90 epithelial ovarian cancer cells co-incubated with ovarian cancer ascites (54). Co-plating with the ovarian cancer ascites correlated with increased cancer cell migration, and several genes, including *LAMP-1*, were identified as being differentially up-regulated during this process, suggesting a potential role in cancer progression. Further, transient transfection studies indicate that PI3K/Akt pathway inactivation by LY294002 had no effect on LAMP-1 cellular expression or lysosomal function in 293T and SKBR-3 cell lines stimulated with EGF (55). These data support our proteomic findings, which suggest that EGF-mediated LAMP-1 stimulation is independent of PI3K/Akt activation.

Although the present study suggests a role for LAMP-1 in predicting hyperproliferation via EGF stimulation, further studies are required for the large-scale validation of the protein as a candidate ovarian cancer marker. Analyses focused on the predictive potential of LAMP-1 in the treatment determination of cancer due to EGFR activation; however, the role of LAMP-1 in cancer progression, and its potential subcellular translocation during cancer progression, might serve in elucidating not only the molecular mechanism of action of the protein in ovarian cancer, but also its potential utility as a biomarker. Nonetheless, the findings illustrated in this study are promising. The implementation of a growth-stimulated cancer cell line system facilitates the identification of potential biomarkers from a temporal perspective. This approach also could be applied to cancer pathologies in other organs using sub-type-specific immortalized cell lines under stimulating or inhibitory conditions.

Acknowledgments—We gratefully acknowledge support from the Mass Spectrometry Facility at the Johns Hopkins University, particularly that of Bob Cole, PhD, Tatiana Boronina, PhD, and Robert O'Meally, who offered technical advice. We also thank Ren-Chin Wu, MD, of the Department of Pathology at the Johns Hopkins University, for performing the analysis of tissue microarray slides.

* This work was supported in part by federal funds from the National Cancer Institute, National Institutes of Health, The Early Detection Research Network (EDRN, U01CA152813) and The Clinical Proteomic Tumor Analysis Consortium (CPTAC, U24CA160036).

S This article contains supplemental material.

§ To whom correspondence should be addressed: Dr. Hui Zhang, Department of Pathology, Johns Hopkins University, 1550 Orleans Street, CRBII, Room 3M-03, Baltimore, MD 21231, USA, E-mail: hzhang32@jhmi.edu.

REFERENCES

1. Jemal, A., Bray, F., Center, M. M., Ferlay, J., Ward, E., and Forman, D. (2011) Global cancer statistics. *CA Cancer J. Clin.* **61,** 69–90
2. Jaffe, E. S., Harris, N. L., Stein, H., and Vardiman, J. W. (2001) *WHO Classification of Tumours. Pathology and Genetics of Tumours of the Breast and Female Genital Organs*, IARC Press, Lyon, France
3. Zhang, Y., Tang, H., Cai, J., Zhang, T., Guo, J., Feng, D., and Wang, Z. (2011) Ovarian cancer-associated fibroblasts contribute to epithelial ovarian carcinoma metastasis by promoting angiogenesis, lymphangiogenesis and tumor cell invasion. *Cancer Lett.* **303,** 47–55
4. Ip, C. K., Cheung, A. N., Ngan, H. Y., and Wong, A. S. (2011) p70 S6 kinase in the control of actin cytoskeleton dynamics and directed migration of ovarian cancer cells. *Oncogene* **30,** 2420–2432
5. Chakravarty, D., Roy, S. S., Babu, C. R., Dandamudi, R., Curiel, T. J., Vivas-Mejia, P., and Lopez-Berestein, G. (2011) Therapeutic targeting of PELP1 prevents ovarian cancer growth and metastasis. *Clin. Cancer Res.* **17,** 2250–2259
6. Tse, J. C., and Kalluri, R. (2007) Mechanisms of metastasis: epithelial-to-mesenchymal transition and contribution of tumor microenvironment. *J. Cell. Biochem.* **101,** 816–829
7. Jechlinger, M., Grunert, S., and Beug, H. (2002) Mechanisms in epithelial plasticity and metastasis: insights from 3D cultures and expression profiling. *J. Mammary Gland Biol. Neoplasia* **7,** 415–432
8. Thiery, J. P. (2002) Epithelial-mesenchymal transitions in tumour progression. *Nat. Rev. Cancer* **2,** 442–454
9. Hynes, N., and MacDonald, G. (2009) ErbB receptors and signaling pathways in cancer. *Curr. Opin. Cell. Biol.* **21,** 177–184
10. Stadlmann, S., Gueth, U., Reiser, U., Diener, P., Zeimet, A., Wight, E., Mirlacher, M., Sauter, G., Mihatsch, M., and Singer, G. (2006) Epithelial

growth factor receptor status in primary and recurrent ovarian cancer. *Mod. Pathol.* **19,** 607–610
11. Dimova, I., Zaharieva, B., Raitcheva, S., Dimitrov, R., Doganov, N., and Toncheva, D. (2006) Tissue microarray analysis of EGFR and erbB2 copy number changes in ovarian tumors. *Int. J. Gynecol. Pathol.* **16,** 145–151
12. Siwak, D., Carey, M., Hennessy, B., Nguyen, C., McGahren Murray, M., Nolden, L., and Mills, G. (2010) Targeting the epidermal growth factor receptor in ovarian cancer: current knowledge and future challenges. *J. Oncol.* **2010,** 568938
13. Brustmann, H. (2008) Epidermal growth factor receptor expression in serous ovarian carcinoma: an immunohistochemical study with galectin-3 and cyclin D1 and outcome. *Int. J. Gynecol. Pathol.* **27,** 380–389
14. Psyrri, A., Kassar, M., Yu, Z., Bamias, A., Weinberger, P., Markakis, S., Kowalski, D., Camp, R., Rimm, D., and Dimopoulos, M. (2005) Effect of epidermal growth factor receptor expression level on survival in patients with epithelial ovarian cancer. *Clin. Cancer Res.* **11,** 8637–8643
15. Sheng, Q., and Liu, J. (2011) The therapeutic potential of targeting the EGFR family in epithelial ovarian cancer. *Br. J. Cancer* **104,** 1241–1245
16. Zhou, L., and Leung, B. S. (1992) Growth regulation of ovarian cancer cells by epidermal growth factor and transforming growth factors alpha and beta 1. *Biochim. Biophys. Acta* **1180,** 130–136
17. Zeineldin, R., Muller, C. Y., Stack, M. S., and Hudson, L. G. (2010) Targeting the EGF receptor for ovarian cancer therapy. *J. Oncol.* **2010,** 414676
18. Murphy, M., and Stordal, B. (2011) Erlotinib and gefitinib for the treatment of relapsed platinum pretreated non-small cell lung cancer and ovarian cancer: a systematic review. *Drug Resist. Updat.* **14,** 177–190
19. Posadas, E., Liel, M., Kwitkowski, V., Minasian, L., Godwin, A., Hussain, M., Espina, V., Wood, B., Steinberg, S., and Kohn, E. (2007) A phase II and pharmacodynamic study of gefitinib in patients with refractory or recurrent epithelial ovarian cancer. *Cancer* **109,** 1323–1330
20. Gunawardana, C. G., Kuk, C., Smith, C. R., Batruch, I., Soosaipillai, A., and Diamandis, E. P. (2009) Comprehensive analysis of conditioned media from ovarian cancer cell lines identifies novel candidate markers of epithelial ovarian cancer. *J. Proteome Res.* **8,** 4705–4713
21. Faca, V. M., Ventura, A. P., Fitzgibbon, M. P., Pereira-Faca, S. R., Pitteri, S. J., Green, A. E., Ireton, R. C., Zhang, Q., Wang, H., O'Briant, K. C., Drescher, C. W., Schummer, M., McIntosh, M. W., Knudsen, B. S., and Hanash, S. M. (2008) Proteomic analysis of ovarian cancer cells reveals dynamic processes of protein secretion and shedding of extra-cellular domains. *PLoS One* **3**(6), e2425
22. Bengtsson, S., Krogh, M., Szigyarto, C. A., Uhlen, M., Schedvins, K., Silfversward, C., Linder, S., Auer, G., Alaiya, A., and James, P. (2007) Large-scale proteomics analysis of human ovarian cancer for biomarkers. *J. Proteome Res.* **6,** 1440–1450
23. Hamilton, T., Young, R., McKoy, W., Grotzinger, K., Green, J., Chu, E., Whang-Peng, J., Rogan, A., Green, W., and Ozols, R. (1983) Characterization of a human ovarian carcinoma cell line (NIH:OVCAR-3) with androgen and estrogen receptors. *Cancer Res.* **43,** 5379–5389
24. Hu, L., Zaloudek, C., Mills, G. B., Gray, J., and Jaffe, R. B. (2000) In vivo and in vitro ovarian carcinoma growth inhibition by a phosphatidylinositol 3-kinase inhibitor (LY294002). *Clin. Cancer Res.* **6,** 880–886
25. Lafky, J. M., Wilken, J. A., Baron, A. T., and Maihle, N. J. (2008) Clinical implications of the ErbB/epidermal growth factor (EGF) receptor family and its ligands in ovarian cancer. *Biochim. Biophys. Acta* **1785,** 232–265
26. Zhang, H., Liu, A. Y., Loriaux, P., Wollscheid, B., Zhou, Y., Watts, J. D., and Aebersold, R. (2007) Mass spectrometric detection of tissue proteins in plasma. *Mol. Cell. Proteomics* **6,** 64–71
27. Tian, Y., Tan, A. C., Sun, X., Olson, M. T., Xie, Z., Jinawath, N., Chan, D. W., Shih, I.-M., Zhang, Z., and Zhang, H. (2009) Quantitative proteomic analysis of ovarian cancer cells identified mitochondrial proteins associated with paclitaxel resistance. *Proteomics Clin. Appl.* **3**(11), 1288–1295
28. Tian, Y., Yao, Z., Roden, R. B., and Zhang, H. (2011) Identification of glycoproteins associated with different histological subtypes of ovarian tumors using quantitative glycoproteomics. *Proteomics* **11,** 4677–4687
29. Kim, J., Coffey, D., Creighton, C., Yu, Z., Hawkins, S., and Matzuk, M. (2012) High-grade serous ovarian cancer arises from fallopian tube in a mouse model. *Proc. Natl. Acad. Sci.* **109,** 3921–3926
30. Tone, A., Salvador, S., Finlayson, S., Tinker, A., Kwon, J., Lee, C., Cohen, T., Ehlen, T., Lee, M., Carey, M., Heywood, M., Pike, J., Hoskins, P., Stuart, G., Swenerton, K., Huntsman, D., Gilks, C., Miller, D., and McAlpine, J. (2012) The role of the fallopian tube in ovarian cancer. *Clin. Adv. Hematol. Oncol.* **10,** 296–306
31. Han, J., Li, L., Hu, J., Yu, L., Zheng, Y., Guo, J., Zheng, X., Yi, P., and Zhou, Y. (2010) Epidermal growth factor stimulates human trophoblast cell migration through rho A and rho C activation. *Endocrinology* **151,** 1732–1742
32. Papaiahgari, S., Yerrapureddy, A., Hassoun, P. M., Garcia, J. G., Birukov, K. G., and Reddy, S. P. (2007) EGFR-activated signaling and actin remodeling regulate cyclic stretch-induced NRF2-ARE activation. *Am. J. Respir. Cell Mol. Biol.* **36,** 304–312
33. den Hartigh, J. C., van Bergen en Henegouwen, P. M., Verkleij, A. J., and Boonstra, J. (1992) The EGF receptor is an actin-binding protein. *J. Cell Biol.* **119,** 349–355
34. Gagne, J. P., Ethier, C., Gagne, P., Mercier, G., Bonicalzi, M. E., Mes-Masson, A. M., Droit, A., Winstall, E., Isabelle, M., and Poirier, G. G. (2007) Comparative proteome analysis of human epithelial ovarian cancer. *Proteome Sci.* **24,** 5–16
35. Fidler, I. J. (1990) Host and tumour factors in cancer metastasis. *Eur. J. Clin. Invest.* **20,** 481–486
36. Sibilia, M., Kroismayr, R., Lichtenberger, B. M., Natarajan, A., Hecking, M., and Holcmann, M. (2007) The epidermal growth factor receptor: from development to tumorigenesis. *Differentiation* **75,** 770–787
37. Vlahos, C. J., Matter, W. F., Hui, K. Y., and Brown, R. F. (1994) A specific inhibitor of phosphatidylinositol 3-kinase, 2-(4-morpholinyl)-8-phenyl-4H-1-benzopyran-4-one (LY294002). *J. Biol. Chem.* **269,** 5241–5248
38. Wieduwilt, M. J., and Moasser, M. M. (2008) The epidermal growth factor receptor family: biology driving targeted therapeutics. *Cell. Mol. Life Sci.* **65,** 1566–1584
39. Mendelsohn, J., and Baselga, J. (2006) Epidermal growth factor receptor targeting in cancer. *Semin. Oncol.* **33,** 369–385
40. Chen, J. W., Murphy, T. L., Willingham, M. C., Pastan, I., and August, J. T. (1985) Identification of two lysosomal membrane proteins. *J. Cell Biol.* **101,** 85–95
41. Granger, B. L., Green, S. A., Gabel, C. A., Howe, C. L., Mellman, I., and Helenius, A. (1990) Characterisation and cloning of lgp110, a lysosomal membrane glycoprotein from mouse and rat cells. *J. Biol. Chem.* **265,** 12036–12043
42. Heffernan, M., Yousefi, S., and Dennis, J. W. (1989) Molecular characterization of P2B/LAMP-1, a major protein target of a metastasis-associated oligosaccharide structure. *Cancer Res.* **49,** 6077–6084
43. Kannan, K., Stewart, R. M., Bounds, W., Carlsson, S. R., Fukuda, M., Betzing, K. W., and Holcombe, R. F. (1996) Lysosome-associated membrane proteins h-LAMP1 (CD107a) and h-LAMP2 (CD107b) are activation-dependent cell surface glycoproteins in human peripheral blood mononuclear cells which mediate cell adhesion to vascular endothelium. *Cell. Immunol.* **171,** 10–19
44. Silverstein, R. L., and Febbraio, M. (1992) Identification of lysosome-associated membrane protein-2 as an activation-dependent platelet surface glycoprotein. *Blood* **80,** 1470–1475
45. Holcombe, R. F., Baethge, B. A., Stewart, R. M., Betzing, K., Hall, V. C., Fukuda, M., and Wolf, R. E. (1993) Cell surface expression of lysosome-associated membrane proteins (LAMPs) in scleroderma: relationship of LAMP2 to disease duration, anti-Sc170 antibodies, serum interleukin-8, and soluble interleukin-2 receptor levels. *Clin. Immunol. Immunopathol.* **67,** 31–39
46. Williams, M. A., and Fukuda, M. (1990) Accumulation of membrane glycoproteins in lysosomes requires a tyrosine residue at a particular position in the cytoplasmic tail. *J. Cell Biol.* **111,** 955–966
47. Dahlgren, C., Carlsson, S. R., Karlsson, A., Lundqvist, H., and Sjolin, C. (1995) The lysosomal membrane glycoproteins LAMP-1 and LAMP-2 are present in mobilizable organelles, but are absent from the azurophil granules of human neutrophils. *Biochem. J.* **311,** 667–674
48. Peters, P. J., Borst, J., Oorschot, V., Fukuda, M., Krahenbuhl, O., Tschopp, J., Slot, J. W., and Geuze, H. J. (1991) Cytotoxic T lymphocyte granules are secretory lysosomes, containing both perforin and granzymes. *J. Exp. Med.* **173,** 1099–1109
49. Krishnan, V., Bane, S. M., Kawle, P. D., Naresh, K. N., Kalraiya, R. D. (2005) Altered melanoma cell surface glycosylation mediates organ specific adhesion and metastasis via lectin receptors on the lung vascular endothelium. *Clin. Exp. Metastasis* **22,** 11–24

50. Inohara, H., and Raz, A. (1994) Identification of human melanoma cellular and secreted ligands for galectin-3. *Biochem. Biophys. Res. Commun.* **201,** 1366–1375
51. Kunzli, B. M., Berberat, P. O., Zhu, Z. W., Martignoni, M., Kleeff, J., Tempia-Caliera, A. A., Fukuda, M., Zimmermann, A., Friess, H., and Buchler, M. W. (2002) Influences of the lysosomal associated membrane proteins (LAMP-1, LAMP-2) and MAC-2 binding protein (MAC-2-BP) on the prognosis of pancreatic carcinoma. *Cancer* **94,** 228–239
52. Spano, J. R., Fagard, R., Soria, J.-C., Rixe, O., Khayat, D., and Milano, G. (2005) Epidermal growth factor receptor signaling in colorectal cancer: preclinical data and therapeutic perspectives. *Ann. Oncol.* **16,** 189–194
53. Seiden, M. V., Burris, H. A., Matulonis, U., Hall, J. B., Armstrong, D. K., Speyer, J., Weber, J. D. A., and Muggia, F. (2007) A phase II trial of EMD72000 (matuzumab), a humanized anti-EGFR monoclonal antibody, in patients with platinum-resistant ovarian and primary peritoneal malignancies. *Gynecol. Oncol.* **104,** 727–731
54. Meunier, L., Puiffe, M. L., Le Page, C., Filali-Mouhim, A., Chevrette, M., Tonin, P. N., Provencher, D. M., and Mes-Masson, A. (2010) Effect of ovarian cancer ascites on cell migration and gene expression in an epithelial ovarian cancer in vitro model. *Transl. Oncol.* **3,** 230–238
55. Chen, X., and Wang, Z. (2001) Regulation of intracellular trafficking of the EGF receptor by Rab5 in the absence of phosphatidylinositol 3-kinase activity. *EMBO Rep.* **2,** 68–74